Water Supply

Water Supply Vol 22 No 9, 7337 doi: 10.2166/ws.2022.296

Modeling the formation of disinfection byproducts in chlorinated swimming pool water: Role of body fluid analog

Pei Hua[a,b,*], Yingjie Chen[a,b] and Jin Zhang[c]

[a] Environmental Research Institute, Guangdong Provincial Key Laboratory of Chemical Pollution and Environmental Safety & MOE Key Laboratory of Theoretical Chemistry of Environment, South China Normal University, 510006 Guangzhou, China
[b] School of Environment, South China Normal University, University Town, 510006 Guangzhou, China
[c] State Key Laboratory of Hydrology-Water Resources and Hydraulic Engineering, Yangtze Institute for Conservation and Development, Hohai University, 210098 Nanjing, China
*Corresponding author. E-mail: pei.hua@m.scnu.edu.cn

ABSTRACT

The recirculation of pool water and the continuous input of pollutants and disinfectants in swimming pools intensifies the accumulation of disinfection byproducts (DBPs), which have received increasing attention. Trihalomethanes (THMs) are the most common DBPs found in swimming pool water. Developing a predictive THM model is an efficient and promising way to optimize the chlorine dosage and guarantee water safety. Because the main components of swimmer inputs and their respective quantities have been formalized and determined through body fluid analogs (BFA), the model development can rely on the chlorination of BFA components and mixtures. In this study, a well-established second-order reaction chlorine decay model with a variable reaction rate coefficient was expanded to describe the chlorine consumption in swimming pool water. The THM model with a variable formation coefficient was first developed based on the identical assumption of the chlorine model, that is, the reactivity of the reactants decreases as the reaction progresses. The results showed that uric acid exhibited the fastest initial rate coefficient for chlorine decay. Although citric acid showed a considerably high specific THM formation potential (μmol-THM, species/mg productive chlorine consumption), urea and humic acid (HA) were attributed to the fast-reacting THM formation precursors. The rate coefficients of urea and HA were higher than that of citric acid. For the mixture, the (overall) reaction rate coefficients were formulated as a function of the rate coefficient of the individual substance and the concentration of the substance remaining in the water. This concept was tested using BFA and BFA with HA. The model accurately described the chlorine consumption and THM concentrations ($R^2 > 0.96$).

Key words: body fluid analog, disinfection byproducts, kinetics model, swimming pool water

HIGHLIGHTS

- BFA is more reactive than HA toward chlorine consumption.
- HA results in more TCM formation than BFA does.
- A variable reaction rate coefficient model for THM formation was developed.
- The rate coefficient of mixtures depends on rate coefficient and concentration of individual substances.

GRAPHICAL ABSTRACT

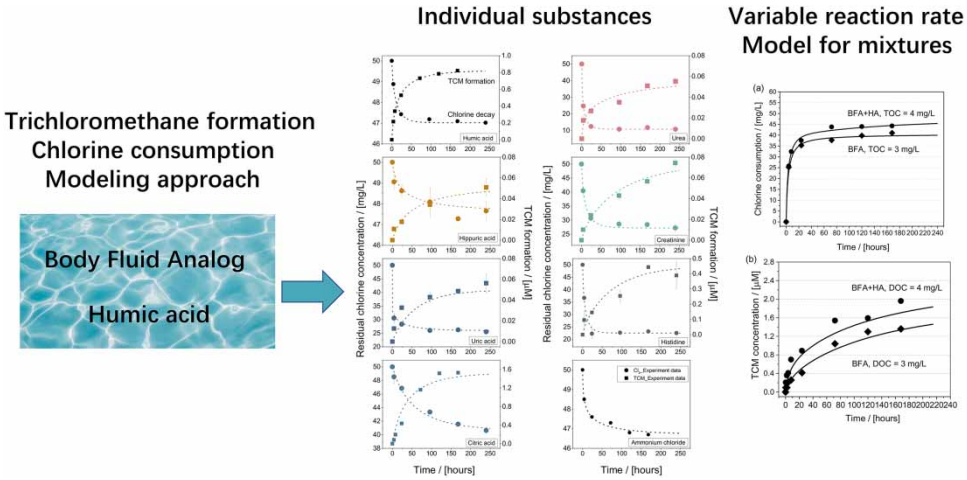

1. INTRODUCTION

Pollutants from pool users are introduced into swimming pool water in the form of body fluids, such as sweat, urea, saliva, and/or suspended particles, such as hair and skin cells, as well as certain synthetic chemicals originating from sunscreen or deodorants (Keuten *et al.* 2012, 2014; Virkutyte *et al.* 2012). The initial input of anthropogenic pollutants can be substantially decreased by thorough pre-swim showering, whereas the continuous input of post-shower pollutants cannot be avoided (Yeh *et al.* 2014). Because of the recirculation of swimming pool water and inefficient conventional pool water treatment, pollutants accumulate and remain in the pool water before the pool is emptied and renovated (Barbot & Moulin 2008; Yeh *et al.* 2014). Seawater or disinfected distributed drinking water is used to refill or partially replace pool water, which is referred to as filling water. Although filling water can dilute the anthropogenic pollutant content, it also introduces natural organic matter (NOM) that remains in freshwater after treatment, and inorganic matter such as bromide, into the swimming pool water (Kanan & Karanfil 2011; Manasfi *et al.* 2016). Chlorine is an input substance that inactivates microorganisms and ensures microbiological safety of swimming pool water. However, chlorine reacts with inorganic matter and NOM originating from swimmers and from filling water, leading to the formation of potentially harmful disinfection byproducts (DBPs) (Zwiener *et al.* 2007; Richardson *et al.* 2010; Chowdhury *et al.* 2014). The exposure risk assessment illustrated that swimming pool water could be more genotoxic than chlorinated tap water, emphasizing the importance of controlling DBPs concentrations in swimming pool water (Plewa *et al.* 2008; Liviac *et al.* 2010).

Among the commonly detected and regulated DBPs, trihalomethanes (THMs) are the predominant species, and one has been studied most intensively. Trichloromethane (TCM) is the main THM compound formed in fresh chlorinated swimming pools, ahead of dibromochloromethane, bromodichloromethane, and tribromomethane (Chu & Nieuwenhuijsen 2002; Chowdhury *et al.* 2014), whereas brominated THMs are important in saline water pools or bromine-disinfected pools (Lourencetti *et al.* 2012). A better understanding of the kinetics of chlorine consumption and THM formation in swimming pool water is helpful for guaranteeing a healthy pool environment. Therefore, a so-called body fluid analog (BFA) was proposed as a surrogate for the chemical composition of micropollutants introduced into swimming pools, which facilitates the following investigation.

The BFA contains several constituents, including urea, uric acid, amino acids, and ammonia chloride, which are mixed at typical ratios to represent the pollutants introduced by pool users (Borgmann-Strahsen 2003; Judd & Bullock 2003; Goeres *et al.* 2004). Efforts have been made to understand the chemistry of the reactions between chlorine and individual BFA constituents, such as urea (Blatchley & Cheng 2010; De Laat *et al.* 2011), uric acid (Lian *et al.* 2014), and organic nitrogen DBP precursors such as creatinine and L-histidine (Li & Blatchley 2007). However, less attention has been paid to the time-course contribution of an individual constituent to chlorine consumption and THM formation in the BFA mixture. Moreover, the results of previous investigations are rarely related to the prediction of chlorine consumption and DBP formation in swimming pool water, particularly when compared with the model simulation for disinfected drinking water.

The formation of THM can be simulated using multiple regression or reaction kinetic approaches. The former was developed using multiple regression analysis of THM concentration, water quality parameters such as total organic carbon (TOC) or dissolved organic carbon (DOC), and operational parameters. However, the application of the multivariate approach may be limited to simulating the dynamic variation in the THM concentration in swimming pool water. This is because the observed fluctuations in THM concentration lag NOM concentration by several days (Peng *et al.* 2016). In other words, the responses of THM formation to the variation of precursors are not simultaneous, as the precursors with low reactivity require a longer reaction time with chlorine. Unlike the multiple regression approach, the kinetic approach is based on a reaction theory that considers the quantity and properties of reactants and has been widely used in the simulation of drinking water quality (Fisher *et al.* 2012, 2021). Therefore, it is reasonable to consider the reactivity of organic THM-precursors in swimming pool water. Currently, the THM species formation model was reported based on the concept that THM-productive chlorine consumption was linearly related to the formation of THM or individual THM species (Sathasivan *et al.* 2020). However, the residual chlorine in swimming pool water is relatively stable while the composition and concentration of precursors are variable depending on the number of swimmers. Therefore, the development of THM formation model for swimming pool water should focus on the reactivity and concentration of reactants.

Consequently, to optimize chlorine dosage and minimize DBPs, the objective of this study was to develop kinetic models for chlorine consumption and THM formation in swimming pool water. The BFA was applied as a surrogate for the micropollutants released by pool users, while humic acid (HA) was used to represent the NOM introduced by the filling water. The BFA and HA mixture was treated as synthetic swimming pool water. The detailed aims were to: (i) determine the specific chlorine demand and specific trihalomethane formation potential (THMFP) of each BFA constituent and HA; (ii) evaluate the time-course contributions of the individual constituents to the chlorine consumption and THM formation of synthetic swimming pool water; (iii) determine the reaction rate coefficients of chlorine consumption and TCM formation for each BFA constituent and HA; and (iv) simulate the kinetics of chlorine consumption and THM formation for the BFA mixture and the BFA and HA mixture based on the proposed models.

2. MATERIAL AND METHODS

2.1. Solution preparation

All reactants were reagent grade chemicals and used without further purification. BFA organic stock solutions were prepared by gravimetrically adding known constituents into purified water and dissolving at pH 12 (NaOH, 2 mol/L) according to the method described by Judd & Bullock (2003), the pH of which was then adjusted to neutral using 1 mol/L sulfuric acid. The composition of the stock BFA solution and the percentages of carbon and nitrogen contributed by individual BFA constituents are listed in Table 1. The HA stock solution was prepared by dissolving sodium salt (Sigma-Aldrich, MO, USA) at pH 12 (NaOH, 2 mol/L) and stirring at 20 °C for ca. 30 h. The solution was adjusted to neutral pH and then filtered through a 0.45 μm polycarbonate filter (Nuclepore Track-Etch Membrane, Whatman, Germany) to remove suspended solids. Dilution of BFA and HA to target aqueous-phase concentrations was accomplished with distilled deionized water (18.2 MΩ•cm at 25 °C; Direct-Q system, Merck Millipore, MA, USA). The BFA and HA mixture, which surrogated the swimming pool water, was labeled as BFA + HA and prepared by mixing and diluting BFA and HA stock solutions to the target concentration. All the solutions were freshly prepared before the chlorination experiments, and the final non-purgeable organic carbon (NPOC) concentrations were measured. A chlorine stock solution (≈15.5 mM) was prepared from a commercial sodium hypochlorite solution (14% active chlorine; VWR, PA, USA). Phosphate buffer (10 mM) was prepared. The chlorine stock and buffer solutions were refrigerated at 4 °C.

2.2. Experimental procedures

2.2.1. Chlorine demand and THM formation potential test

The NPOC concentration of organic samples was fixed at 2 mg/L to study the specific chlorine demand and specific THMFP of the individual BFA constituents and HA. Chlorination was performed using 300 mL brown glass bottles. The glassware was pre-soaked in a dilute chlorine bath (≈2 mM) for at least 15 h and then rinsed with purified water before the chlorination experiments (De Laat *et al.* 2011). All samples were maintained at pH 7.2 with phosphate buffer before chlorination. To allow the chlorine reaction to approach completion, an appropriate volume of chlorine stock solution was spiked into individual samples to achieve an initial chlorine concentration (ICC) of 50 mg/L. It should be illustrated that the chlorine concentration of swimming pool water is adjusted and maintained at an adequate level ranging from 0.3 to 2.0 mg/L in

different countries and regions, which are dependent upon several factors such as pool type, the number of people in the pool, temperature, and pH (Barbot & Moulin 2008; Long *et al.* 2019). The chlorine in the gas or liquid form is continuously added to the swimming pool to guarantee enough chlorine residual, thus, it has difficulty conducting re-chlorination under laboratory conditions. To make sure the chlorine concentration is not a limitation for reaction, i.e., enough chlorine remains in the water sample at the end of maximum reaction time, a high initial dosage of 50 mg/L was applied. The chlorinated samples were then immediately hermetically closed and incubated in head-space free glass bottles at 28 ± 1 °C. After 168 h, the residual chlorine was measured, and the remaining sample was quenched by the addition of sodium thiosulfate solution for further TCM measurements.

2.2.2. Kinetics experiments

Two independent experiments were conducted to study the kinetics of chlorine decay and THM formation. Experiment series were performed to investigate the time-course contribution of individual BFA constituents to chlorine consumption and THM formation of BFA. Therefore, the NPOC of BFA was initially set at 3 mg/L, and the theoretical values of NPOC, nitrogen, and solution concentrations of each BFA constituent were calculated according to the receipt (Table 1). In other words, the NPOC concentration of BFA is a summation of the carbon contributed by the individual BFA constituents. Chlorination of each BFA constituent and BFA was conducted according to their respective NPOC concentrations, as shown in experiment series I (Table 2). Similar experiments were performed using the same procedures as those for the chlorine demand and TCM formation potential tests, however, the reaction times were 4, 24, 72, 120, and 168 h.

Experiment series II was conducted to determine the reaction rate coefficients of individual BFA constituents and HA. Therefore, all organic substances were designed to have an identical NPOC at 2 mg/L, as shown in experiment series II (Table 1). Chlorination experiments were conducted using the same procedures as those used for experiment series I. Eventually, the chlorine consumption and THM formation dataset of synthetic swimming pool water was obtained, including the mixture of BFA and HA at different mixing ratios. An ICC of 50 mg/L was selected for the chlorination experiments. The pH was fixed at 7.2 ± 0.1, and the temperature was maintained at 28 ± 1 °C.

2.3. Analytical methods

The free chlorine concentration was determined according to the N, N-diethyl-p-Phenylenediamine (DPD) Standard Colorimetric Method 4500-Cl G (APHA 2005). The chlorine stock solution was periodically standardized using the DPD method. The NPOC concentration was measured using a TOC-VCPH (Shimazu, Kyoto, Japan). A pH meter 340i (Wissenschaftlich-

Table 1 | Carbon and nitrogen concentrations of individual BFA components, and their corresponding contribution percentages to the BFA (mixture)

Substances	Concentration (mg/L)	Carbon (mg/L)	Carbon percentage contribution (%)	Nitrogen (mg/L)	Nitrogen percentage contribution (%)	Supplier and grade
Urea	14,800	2960	51.48	6900	85.17	Merck Millipore
L-histidine	1210	560	9.74	320	3.95	Alfa Aesar, 98%
Hippuric acid	1710	1040	18.09	134	1.65	Alfa Aesar, 98%
Uric acid	490	180	3.13	160	1.98	Alfa Aesar, 99%
Citric acid	640	240	4.17	NA	NA	Alfa Aesar, 99%
Creatinine	1800	770	13.39	67	0.83	Alfa Aesar, 98%
Ammonia	2000	NA	NA	520	6.42	Merck Millipore
BFA	NA	5750	100	8101	100	NA

Note: The theoretical values of concentration, carbon, and nitrogen are those from Judd & Bullock (2003). NA indicates no contribution.

Table 2 | Experimental design

	Experiment series I			Experiment series II		
Substance	DOC mg/L	Total nitrogen mg/L	Solution concentration μmol/L	DOC mg/L	Total nitrogen mg/L	Solution concentration μmol/L
Urea	1.54	3.59	128.20	2.00	4.66	166.68
L-histidine	0.29	0.17	4.03	2.00	1.17	27.78
Hippuric acid	0.54	0.07	5.00	2.00	0.26	18.52
Uric acid	0.09	0.08	1.50	2.00	1.87	33.33
Citric acid	0.13	NA	1.80	2.00	NA	27.78
Creatinine	0.40	0.35	8.33	2.00	0.74	41.67
Ammonia	NA	0.27	19.41	NA	0.27	19.41
BFA	3.00	NM	NM	NC	NC	NC
Humic acid	1.00	NM	NM	NC	NC	NC
BFA + HA	4.00	NM	NM	NC	NC	NC

Note: NA indicates no contribution; NM indicates not measured; NC indicates not conducted.

Technische-Werkstätten, Weilheim, Germany) was used to measure pH. THM concentrations were determined using a membrane inlet mass spectrometer (MIMS) 2000 (Mikrolab Aarhus, Højbjerg, Denmark), which comprised a Prisma QME 220 PT mass spectrometer (Pfeiffer Vacuum, Asslar, Germany) equipped with electron ionization. THM standards were purchased from Sigma-Aldrich. Before measurement, THM without purification was diluted with ultrapure water to the target solution concentrations and measured for MIMS calibration. Water samples were first analyzed in the mass spectrum scan mode (49-m/z-215). Then, the THM concentration was quantified using selected ion monitoring. Because all the synthesized samples were prepared with ultrapure water, which does not contain bromide, only TCM was detected in all the THM species. Ions at m/z 83 were chosen to quantify TCM, with a quantification limit of 2.5 μg/L. More detailed operation conditions for the MIMS can be found in the literature (Shang & Blatchley 1999; Yang *et al.* 2012).

2.4. Modeling

2.4.1. Reaction rate of individual BFA constituents

Second-order kinetic models were applied to simulate chlorine decay and TCM formation for individual BFA constituents and HA. By employing the derived rate coefficients, the reactivity of the individual substances can be quantitatively discussed. In this study, a second-order model with a variable reaction rate coefficient (VRRC) was applied, as follows (Hua *et al.* 2015):

$$-\frac{dc_{Cl}}{dt} = R_{Cl} = k_{cl}(t) \cdot c_{Cl}(t) \cdot c_{R,Cl}(t) = \alpha \cdot exp^{-\beta \cdot \left[\frac{\Delta c_R(t)}{c_{Cl,max}}\right]} \cdot c_{Cl}t \cdot c_{R,Cl}(t) \quad (1)$$

The underlying assumption is that the reaction rate coefficient $k_{cl}(t)$ is not a constant but varies with the reaction progress owing to the different phases of the reaction; thus, the decay model is referred to as a VRRC, where α [L/mg/h] and β [dimensionless] are the model parameters for $k_{cl}(t)$; $c_{cl}(t)$ [mg/L] is the chlorine concentration; $c_{R,Cl}(t)$ [mg/L] is the reactant concentration at time t; $c_{cl,max}$ is the maximum chlorine demand, that is, $c_{cl,max} = c_R(0)$. $\Delta c_{R,Cl}(t)$ is the consumed reactant concentration at time t; thus, $c_{R,Cl}(t) = c_{R,Cl}(0) - \Delta c_{R,Cl}(t)$. Based on the principle of mass conservation and the hypothesis that the stoichiometric coefficient for chlorine and the reactant is equal to one, the consumed reactant $\Delta c_{R,Cl}(t)$ is equal to $\sum_{t=0}^{t} [R_{Cl}(t) \cdot \Delta t]$ based on the Euler method. Finally, the $c_{R,Cl}(t) = c_{cl,max} - \sum_{t=0}^{t} [R_{Cl}(t) \cdot \Delta t]$.

In this study, Equation (1) was applied to simulate the chlorine decay of each (individual) BFA component as well as HA. In other words, model parameters α and β were derived for each reactant, and the corresponding VRRC for each reactant was

calculated as follows:

$$k_{Cl,i}(t) = \alpha_i \cdot exp^{-\beta_i \cdot \left[\frac{\Delta c_{R,i}(t)}{c_{Cl,max,i}}\right]} \tag{2}$$

where $k_{Cl,i}(t)$ represents the chlorine rate coefficient for the ith reactant/BFA constituent ($i = 1$–8, including seven BFA constituents and HA). α_i and β_i are the model parameters for the ith reactant/BFA constituent, and $c_{cl,max,i}$ is the maximum chlorine demand of an individual substance.

TCM formation models based on fundamental reaction kinetics are able to reduce uncertainty in their prediction (Chowdhury *et al.* 2009). Similar to the chlorine decay model, a second-order TCM formation model was proposed:

$$\begin{aligned}\frac{dc_{TCM}(t)}{dt} = R_{TCM} &= k_{TCM}(t) \cdot c_{Cl}(t) \cdot [c_{TCMFP} - c_{TCM}(t)] \\ &= \gamma \cdot exp^{-\theta \cdot \left[\frac{c_{TCM}(t)}{c_{TCMFP}}\right]} \cdot c_{Cl}(t) \cdot [c_{TCMFP} - c_{TCM}(t)]\end{aligned} \tag{3}$$

where $k_{TCM}(t)$ is the variable-rate coefficient of TCM formation; $c_{TCM}(t)$ is the TCM concentration at time t in μmol/L; c_{TCMFP} [μmol/L] is the TCM formation potential, indicating the maximum concentration of the reactants. γ [L/μmol/h] and θ [dimensionless] are the model parameters for $k_{cl}(t)$. Therefore, the reactant concentration toward TCM formation at time t was defined as $c_{R,TCM} = c_{TCMFP} - c_{TCM}(t)$. $c_{cl}(t)$ is the simulated chlorine concentration obtained using Equation (1). The kinetics of TCM formation for the individual BFA constituents and HA were simulated using Equation (3). Therefore, the rate coefficient of TCM formation for each reactant was determined, namely $k_{TCM,i}(t)$:

$$k_{TCM,i}(t) = \gamma_i \cdot exp^{-\theta_i \cdot \left[\frac{c_{TCM,i}(t)}{c_{TCMFP,i}}\right]} \tag{4}$$

2.4.2. Reaction rate of synthetic swimming pool waters

Synthetic swimming pool water was represented as a mixture of BFA and HA (BFA + HA). It was assumed that the reactions of the individual BFA components and HA proceeded independently in the mixture. Therefore, the overall rate coefficient of the mixture can be expressed as a function of the rate coefficient of the individual substances, as shown in Equation (5):

$$k_{Cl,mix}(t) = \frac{\sum_{i=1}^{m} [k_{Cl,i}(t) \cdot c_{R,i}(t)]}{\sum_{i=1}^{m} c_{R,i}(t)} \tag{5}$$

$$k_{TCM,mix}(t) = \frac{\sum_{i=1}^{m} [k_{TCM,i}(t) \cdot c_{TCM,i}(t)]}{\sum_{i=1}^{m} c_{R,i}(t)} \tag{6}$$

where $k_{Cl,mix}(t)$ and $k_{TCM,mix}(t)$ are the chlorine and TCM rate coefficients for the synthetic swimming pool water (mixture), respectively; $k_{Cl,i}(t)$ and $k_{TCM,i}(t)$ are obtained through model calibration by applying Equations (2) and (4). i represents the individual reactants, ranging from one to eight; where $m = 7$ indicates that the BFA mixture was considered, whereas $m = 8$ indicates that BFA + HA was considered. Therefore, chlorine decay and TCM formation of the mixture can be

calculated as follows:

$$-\frac{dc_{Cl}}{dt} = k_{Cl,mix}(t) \cdot c_{Cl}(t) \cdot c_{R,Cl}(t) \tag{7}$$

$$\frac{dc_{TCM}(t)}{dt} = k_{TCM,mix}(t) \cdot c_{Cl}(t) \cdot [c_{TCMFP} - c_{TCM}(t)] \tag{8}$$

2.5. Model calibration and statistical analysis

Data obtained from experiment series II were used to determine the best-fit parameters of α [L/mg/h] and β toward chlorine decay, as well as γ [L/μmol/h] and θ toward TCM formation for each substance. Excel Solver, which uses the generalized reduced-gradient algorithm, was used to solve Equations (1) and (3) to obtain the model parameters for each substance. They were calculated numerically with a 0.5 h time interval by minimizing the sum of the squared errors between the experimentally determined chlorine or TCM concentrations and simulations at corresponding times. Once the best-fit parameters were determined, the rate coefficients of the mixtures were calculated using Equations (5) and (6). Furthermore, the kinetics of chlorine decay and TCM formation with respect to the mixtures were predicted using Equations (7) and (8) with a 0.5 h time interval.

The accuracy of the model simulation was evaluated using the coefficient of determination (R^2) and root-mean-square error (RMSE). These methods are frequently used as measures of model adequacy and describe the difference between the predicted data and those obtained experimentally (Piñeiro *et al.* 2008). The RMSE evaluates the prediction capability of the model, with a smaller RMSE value indicating a greater predictive capability. The obtained RMSE is also expected to be of a similar magnitude as the measurement error, which indicates a reasonable fit.

3. RESULTS AND DISCUSSION

3.1. Chlorine consumption

3.1.1. Specific chlorine demand

A chlorine demand test was performed to evaluate the reactivity of the investigated substances toward chlorine consumption. Experiment datasets were interpreted in the form of the DOC-related specific chlorine demand (mg Cl_2/mg C) and the solution concentration-related chlorine demand (mol Cl_2/mol BFA component).

The DOC-related specific chlorine demand is shown in Figure 1(a). The specific chlorine dose shown on the horizontal axis was calculated as ICC divided by the initial DOC of the individual BFA components (ICC/DOC, mg Cl_2/mg C). The DOC-related specific chlorine demand increased with an increasing specific chlorine dose and plateaued at specific chlorine doses >20 mg Cl_2/mg C. Urea exhibited the highest demand of 19.5 mg Cl_2/mg C, followed by L-histidine with 13.5 mg Cl_2/mg C, and uric acid with 12.0 mg Cl_2/mg C. These are organic nitrogen compounds, which could reasonably explain the higher DOC-related specific chlorine demand.

The concentration-related chlorine demand is shown in Figure 1(b). The horizontal axis shows the ratios of ICC to the initial solution concentration of the individual BFA components, which are referred to as the specific chlorine doses (ICC/solution concentration, mol Cl_2/mol BFA component). This shows that the specific chlorine demand plateaued at chlorine doses > 20 mol Cl_2/mol BFA. The highest specific chlorine demand was observed for L-histidine, which reached 14 mol Cl_2/mol histidine, followed by uric acid with 10.5 mol Cl_2/mol, and creatinine with 7.5 mol Cl_2/mol. These results can be explained by the structure of the compounds, that is, the more electron-donating functional groups (-NH_2 and -OH) and double bonds in the structure, the higher the chlorine demand (Hong *et al.* 2009). Specifically, L-histidine and creatinine, which contain an aromatic ring and functional group of -NH_2, showed a higher specific chlorine demand than that of hippuric acid, which has no functional groups on its ring and therefore has the lowest demand. The demand for urea was 3.3 mol Cl_2/mol urea, which falls within the theoretical chlorine demand that ranges between 3 and 8 mol Cl_2/mol of urea (De Laat *et al.* 2011).

The data shown in Figure 1(c) are the DOC-related specific chlorine demands of $\sum_7$BFA and HA. $\sum_7$BFA reached the highest plateau level of 14 mg Cl_2/mg C. However, HA was exhibited at 3 mg Cl_2/mg C, which was nearly five times lower than that of BFA. This result agrees with the conclusions reported by Kanan & Karanfil (2011) that BFA is more reactive than HA toward chlorine consumption.

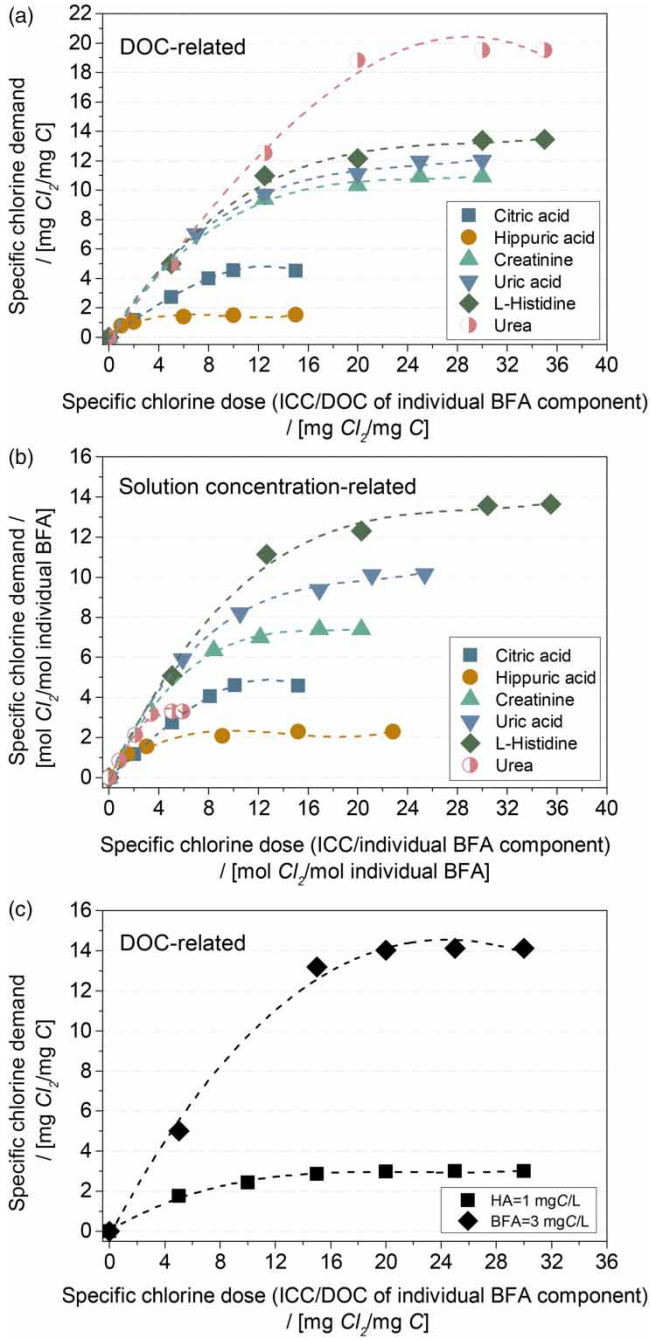

Figure 1 | (a) DOC-related and (b) solution concentration-related specific chlorine demand of organic BFA components, and (c) DOC-related specific chlorine demands of $\sum$7BFA and HA. Tests were performed with 168 h, pH = 7.2 $\pm$ 0.1. Solid line represents the trend of polynomial approximation.

3.1.2. Kinetics of chlorine decay for individual substances

Based on the results of experiment series I (Table 2), the time-course chlorine consumption for seven BFA components and HA with their respective DOC concentrations is shown in Figure 2. The chlorine consumption of urea was significantly higher than that of other substances over the entire reaction period. This is because urea accounted for the highest percentage of $\sum_7$BFA DOC (38.61%, Table 1) and showed the highest DOC-related specific chlorine demand. Conversely, hippuric

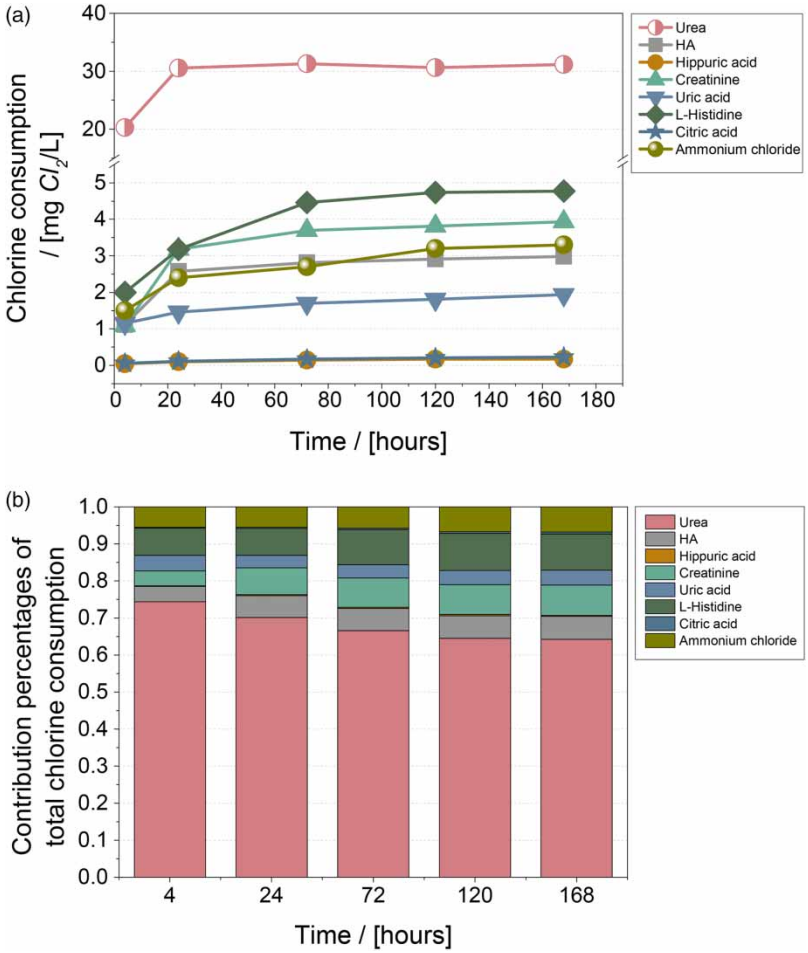

Figure 2 | (a) Time-course chlorine consumption of individual BFA components with their respective initial DOC (Table 2, experiment series I), HA (DOC = 1 mg C/L), and (b) Time-course contribution percentages of individual substances to the chlorine consumption of BFA + HA.

acid showed substantially low chlorine consumption, although it had the second-highest DOC concentration. This result agrees with the findings presented in Figure 1 that hippuric acid exhibits the lowest DOC-related specific chlorine demand.

The chlorine consumption of urea plateaued at 24 h, whereas the consumption of L-histidine increased with increasing reaction time and plateaued at 120 h. These results indicate that individual substances show different reactivity to chlorine and therefore play different roles in the kinetic chlorine consumption of the mixture. For a clearer illustration, time-course contribution percentages were calculated, that is, the chlorine consumption of individual substances divided by the summation of all substance consumption (total consumption) at the corresponding time, as shown in Figure 2(b).

Urea contributed 78.9% to the total consumption at 4 h, while it was 70.4% at 168 h. Uric acid also showed slight decreasing percentages, that is, from 4.5% at 4 h to 4.3% at 168 h. The decreasing percentages may indicate that urea and uric acid were responsible for the total chlorine consumption in the early phase of the reaction. Conversely, the total chlorine consumption contributed by creatinine, HA, and L-histidine increased until 72 h and remained fairly stable until 168 h, indicating that they were responsible for the total chlorine consumption in the later reaction phase. Therefore, the reactivity of chlorine with creatinine, HA, and L-histidine may be slower than that with urea. These hypotheses are further discussed in Section 3.1.3 by deriving their respective reaction rate coefficients.

3.1.3. Chlorine decay rate coefficient for individual substances

To determine the chlorine decay reaction rate coefficient for each substance, the proposed model (Equation (1)) was applied individually to the decay dataset obtained from experiment series II. The chlorine demand $c_{cl,max,i}$ of i^{th} reactant, as required

by Equation (2), was calculated as the DOC concentration of an individual substance (DOC = 2 mg/L, experiment series II) multiplied by their corresponding specific chlorine demand (Figure 1(b)). The best-fit parameters of α_i and β_i for each substance were obtained by curve fitting. The variable reaction rate coefficient $k_{Cl,i}(t)$ of chlorine with respect to the ith reactant was calculated using Equation (2). The values of the best-fit parameters α_i and β_i, chlorine demand $c_{cl,max,i}$ and rate coefficient $k_{Cl,i}(t)$ are listed in Table 3.

Based on Equation (2), α_i is equal to the initial $k_{Cl,i}(0)$, indicating α reflects the initial reaction rate when $\Delta c_{R,i}(t) = 0$. Uric acid exhibited the highest $\alpha_{uric\ acid}$, which is consistent with the conclusions in the literature that uric acid appears to consume free chlorine faster than most other organic-N precursors (Li & Blatchley 2007; Lian *et al.* 2014). Ammonium chloride and urea showed the second and third highest values of α_i, respectively, which were an order of magnitude lower than $\alpha_{uric\ acid}$. The calculated α_{urea} confirmed the assumption derived from the results of experiment series I, that is, the reactivity of chlorine with urea may be faster than that of creatinine, HA, and L-histidine. α values of hippuric acid and citric acid showed the lowest reactivity toward chlorine consumption compared with that of the other BFA components.

Figure 3 shows the measured datasets and curve fitting results for all substances. Except for a few data points, the chlorine decay of the substances was reasonably described by the curve. Table 3 summarizes the results of the model evaluation. R^2 ranges from 0.96 to 0.99 and RMSE were observed from 0.1 to 1.0 mg/L, indicating the model successfully simulated the experimental datasets.

3.1.4. Prediction of chlorine decay of mixtures

As the model parameters α_i and β_i for the individual substances were determined, the reaction rate coefficients for the mixture $k_{Cl,mix}(t)$ could be calculated according to Equation (5). Subsequently, the kinetics of chlorine decay with respect to the mixtures of BFA and BFA + HA were predicted by applying Equation (7). Chlorine consumption is a more important factor than residual chlorine concentration in pool water, as the latter should remain constant to ensure microbial safety. Therefore, the time-course chlorine consumption was calculated as ICC of 50 mg/L minus the residual chlorine concentration at the corresponding time, which is shown in Figure 4(a). The chlorine consumption profiles of both BFA and BFA + HA follow the same pattern, which is characterized by an initial fast consumption stage and a later slower formation stage. Figure 4(a) also shows the prediction results of chlorine consumption for BFA and BFA + HA as a function of time. Graphically, the model results show a good simulation. Quantitatively, the value of R^2 for the model accuracy evaluation was 0.99, that is,

Table 3 | Best-fit model parameters α and β, overall reaction rate coefficient of chlorine decay, chlorine demand, and corresponding R^2 and RMSE with respect to individual substances and substance mixture

Substance (i)	α_i L/mg/h	β_i	$k_{Cl,i}(t)$ L/mg/h	$c_{cl,max,i}$ mg/L	R^2	RMSE mg/L
Uric acid	2.81×10^{-2}	3.85	2.81E-2–6.06×10^{-4}	24.50	0.983	0.501
Urea	6.73×10^{-3}	0.14	6.73E-3–5.85×10^{-3}	39.00	0.994	0.576
L-histidine	4.22×10^{-3}	0.32	4.22E-3–3.07×10^{-3}	27.48	0.966	1.074
Creatinine	2.85×10^{-3}	0.59	2.85E-3–1.58×10^{-3}	22.79	0.990	0.856
Humic acid	2.81×10^{-3}	0.97	2.81E-3–1.07×10^{-3}	2.98	0.992	0.080
Hippuric acid	1.39×10^{-3}	2.30	1.39E-3–2.57×10^{-4}	2.34	0.874	0.345
Citric acid	4.25×10^{-4}	0.41	4.25E-4–2.87×10^{-4}	9.25	0.979	0.481
Ammonia	7.10×10^{-3}	3.67	7.10E-3–1.94×10^{-4}	3.30	0.964	0.123
Mixture	α	β	$k_{Cl,mix}(t)$	$c_{cl,max}$	R^2	RMSE
	L/mg/h		L/mg/h	mg/L		mg/L
BFA	–	–	6.52E-3–2.88×10^{-4}	42.20	0.994	1.122
BFA + HA	–	–	6.30E-3–9.20×10^{-4}	47.35	0.994	1.155

Note: the range of $k_{cl}(t)$ indicates the changes of rate coefficient from $t = 0$ h to $t = 240$ h; DOC of individual substance and HA were 2 and 1 mg/L, respectively; DOC of BFA ($\sum_7$BFA) was 3 mg/L while it of BFA + HA was 4 mg/L.

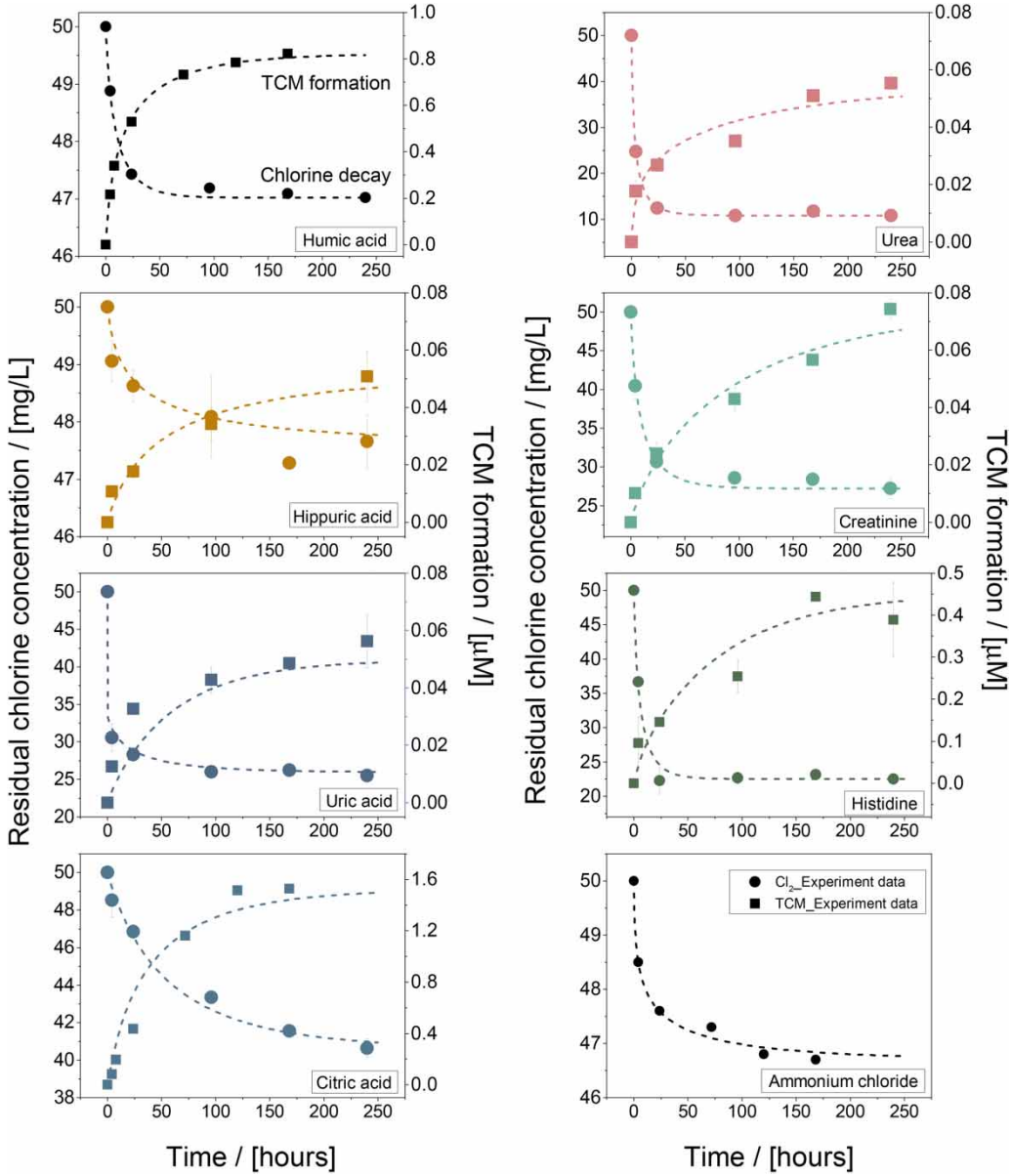

Figure 3 | Curve fitting for individual BFA components and HA with respect to chlorine decay and TCM formation.

1% of the variance was unexplained. RMSE was 1.12 for BFA while 1.16 mg/L for BFA + HA. These results prove that the model provides an excellent prediction of the experimental data.

3.2. Trichloromethane formation

3.2.1. Specific trichloromethane formation potential

As all the synthesized samples were prepared with ultrapure water, which does not contain bromide, only TCM was detected in all the THM species. Specific TCMFP was calculated as TCMFP divided by the corresponding DOC concentration (μmol TCM/mg C). Citric acid exhibited considerably higher specific TCMFP at 10.6 μmol/mg C than that of all the other individual BFA components despite its low chlorine consumption. HA showed the second-highest value of specific TCMFP at 0.82 μmol/mg C, which was approximately 2.5 times higher than that of BFA at 0.45 μmol/mg C. This indicates that HA resulted in more TCM formation than BFA did. Therefore, controlling the organic precursor in the filling water is helpful in decreasing TCM formation in pool water.

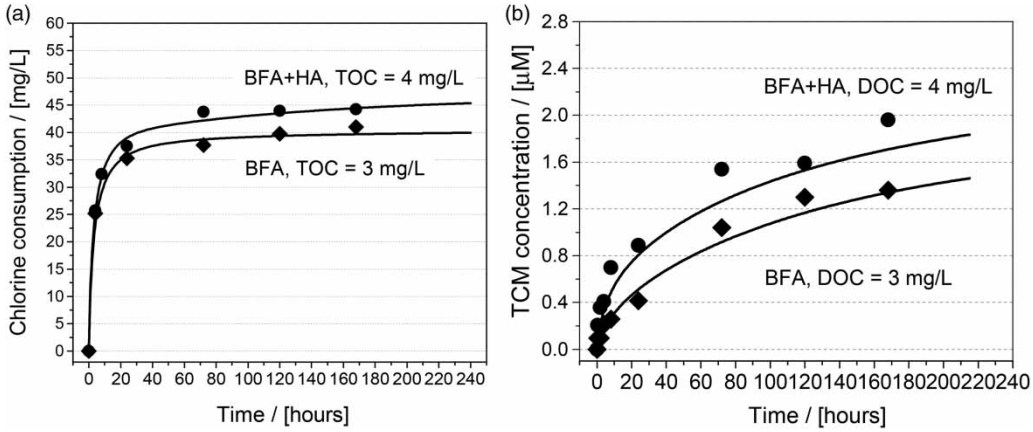

Figure 4 | Chlorine decay experiment and model simulation results for BFA and BFA with HA.

3.2.2. Kinetic TCM formation of substances with individual DOC concentration

Based on the results obtained from experiment series I (Table 2), Figure 5(a) presents the TCM formation as a function of time with regards to organic BFA components and HA with their individual DOC concentrations. Citric acid showed the highest TCM formation, followed by HA, which was consistent with the results of the TCMFP test. Moreover, the TCM formation of citric acid increased until 120 h, whereas that of HA plateaued at 24 h. These results indicate that the substances exhibited different reactivities toward TCM formation, and therefore may contribute differently to the TCM formation of the mixture. Similar to the interpretation of the chlorine consumption results, the time-course contribution percentage of the TCM formation was calculated. These were calculated as the TCM concentration of individual substances to the summation of the TCM formation of all substances (total TCM) at the corresponding time (Figure 5(b)).

Although citric acid contributed the least to chlorine consumption, over 50% of the total TCM was formed due to the presence of citric acid. Approximately 90% of total TCM formation was attributed to the presence of citric acid and HA. Urea, hippuric acid, and creatinine were responsible for 64% of the total DOC of BFA + HA whereas <10% of TCM formation was caused by these components. Moreover, the time-course contribution of HA and citric acid to total TCM formation showed an adverse trend. Specifically, the contribution percentage of HA decreased, while that of citric acid increased with increasing

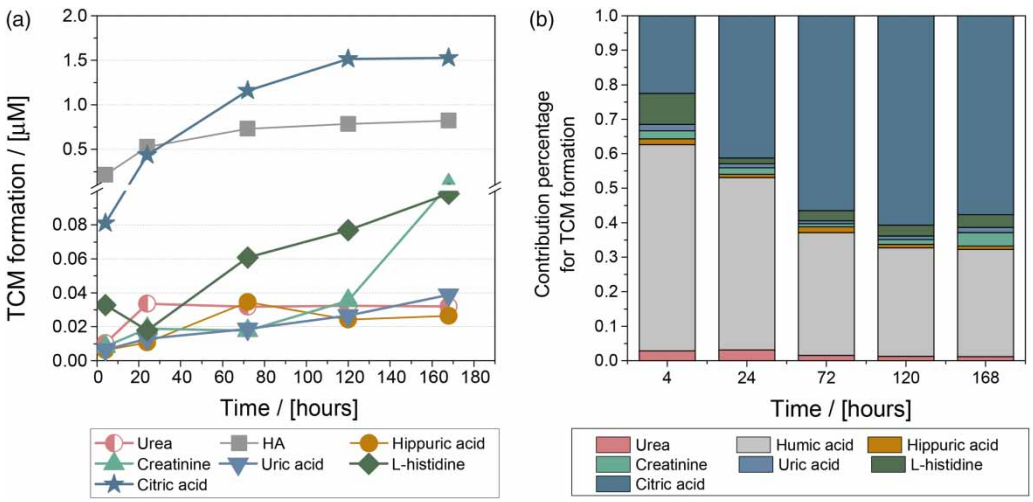

Figure 5 | (a) Time-course TCM formation of individual BFA components with their respective DOC (Table 2 experiment series I), HA (DOC = 1 mg C/L), and (b) Time-course contribution percentages of individual substances to the total TCM formation.

reaction time. This suggests that HA may be responsible for total TCM formation in the early phase of the reaction. This hypothesis was further confirmed by deriving reaction rate coefficients.

3.2.3. Reaction rate coefficient of TCM formation for individual substances

The proposed model (Equation (3)) was applied to each TCM formation dataset of an individual substance obtained from experiment series II. The best-fit parameters of γ [L/μmol/h] and θ were determined by curve fitting, as shown in Figure 3. The $c_{TCMFP,i}$ of individual substance i was experimentally determined. The variable reaction rate coefficient of TCM formation $k_{TCM,i}(t)$ was calculated by applying the best-fit parameters to Equation (4). The values of the best-fit parameters, $c_{TCMFP,i}$ and $k_{TCM,i}(t)$ are shown in Table 4.

As shown, γ is equal to the initial $k_{TCM,i}(0)$, which indicates that γ reflects the initial rate coefficient at $t = 0$. Urea showed the highest initial rate coefficient, followed by HA, which was an order of magnitude higher than those of the other BFA components. Moreover, the initial γ_{HA} was higher than that of citric acid, which agrees with the observations and assumptions obtained from experiment series I (Section 3.2.2), that is, HA may have a higher reactivity toward TCM formation than citric acid does. Although citric acid exhibited the highest specific TCMFP, its rate coefficient was not the highest. This implies that citric acid may be responsible for TCM formation at the slow phase when the circulation time of swimming pool water is long. Moreover, citric acid and histidine show the rate constant ($\theta = 0$), while HA shows the higher θ value indicating the HA rate coefficient varied with reaction time. This may be due to the heterogeneous characteristics of HA. HA contains different reactive sites compared with citric acid and histidine.

The goodness of curve fitting is shown in Figure 4 for the TCM formation of all substances. Graphically, the model accurately describes the experimental data. The values of R^2 ranged from 0.89 to 0.99, indicating a moderate to good simulation (Table 4). The RMSE was observed to range from 0.004 to 0.17 μmol/L. These results indicated that the model successfully simulated the experimental datasets.

3.2.4. Prediction of TCM formation for mixtures

As the model parameters γ_i and θ_i for individual substances are determined, the reaction rate coefficients for substance mixture $k_{TCM,mix}(t)$ can be calculated according to Equation (6). Then, the kinetics of TCM formation with respect to BFA and BFA + HA can be predicted by applying Equation (8). The TCMFP used for model prediction is shown in Table 4.

Figure 4(b) shows the experimental and predicted TCM formation results for BFA and BFA + HA as a function of time. The TCM formation profiles are characterized by an initial fast consumption stage and a later slower formation stage. A good to moderate agreement of TCM concentration was found between experimental data and model predictions for BFA and BFA + HA with R^2 values of 0.98 and 0.95, respectively. Although the RMSE ranged from 0.07 to 0.12 μmol/L,

Table 4 | Best-fit model parameters γ and θ, reaction rate coefficient of TCM formation, TCM formation potential, and corresponding R^2 and RMSE with respect to individual substances and mixture

Substance (i)	γ_i L/μmol/h	θ_i	$k_{TCM,i}(t)$ L/μmol/h	$c_{TCMFP,i}$ μmol	R^2	RMSE μmol/L
Uric acid	7.83×10^{-5}	0.95	7.83E-5–3.11×10^{-5}	0.06	0.964	0.004
Urea	1.69×10^{-4}	1.53	1.69E-4–4.18×10^{-5}	0.05	0.902	0.005
L-histidine	3.92×10^{-5}	0.00	3.92E-5–3.92×10^{-5}	0.39	0.896	0.050
Creatinine	2.88×10^{-5}	0.35	2.88E-5–2.10×10^{-5}	0.07	0.956	0.005
Humic acid	1.33×10^{-4}	1.70	1.33E-4–2.44×10^{-5}	0.82	0.997	0.010
Hippuric acid	3.73×10^{-5}	1.33	3.73E-5–1.11×10^{-5}	0.05	0.947	0.004
Citric acid	5.72×10^{-5}	0.00	5.32E-5–5.32×10^{-5}	19.70	0.948	0.176
mixture	γ L/μmol/h	θ	$k_{TCM,mix}(t)$* L/μmol/h	$c_{TCMFP,mix}$ μmol	R^2	RMSE μmol/L
BFA	–	–	5.55E-5–4.89×10^{-5}	1.72	0.981	0.069
BFA + HA	–	–	8.36E-5–6.95×10^{-5}	2.54	0.959	0.124

Note: the range $k_{TCM,i}(t)$ and $k_{TCM,mix}(t)$ indicate the changes of rate coefficient from $t = 0$ h to $t = 240$ h; the γ and θ for substance mixture are calculated.

it falls in typical precision with 5% error. Thus, graphical and quantitative analyses confirmed an accurate fit to the experimental data.

4. CONCLUSIONS

This study investigated the reactivity of substances remaining in swimming pool waters toward chlorine consumption and TCM formation. Kinetic experiments were conducted to derive the rate coefficients of individual substances. Based on the obtained individual rate coefficients, the proposed models were used to simulate the chlorine consumption and TCM formation of substance mixtures, that is, BFA (mixture) and a BFA and HA mixture (BFA + HA).

The results showed that urea exhibited the highest DOC-related specific chlorine demand, which is attributed to its higher nitrogen concentration than other BFA components. BFA was more reactive than HA toward chlorine consumption. However, the specific TCMFP of HA was approximately 2.5 times higher than that of BFA, indicating that HA is more reactive toward TCM formation. Citric acid showed a considerably higher specific TCMFP than other BFA components. Uric acid exhibited the fastest initial rate coefficient of chlorine decay, which was an order of magnitude higher than those of hippuric and citric acids. Regarding TCM formation, urea and HA were attributed to the fast-reacting TCM formation precursors, which were a magnitude higher than that of citric acid.

For substance mixtures, a hypothesis was proposed to calculate the (overall) rate coefficient, that is, the rate coefficients of the mixture depend on the rate coefficient of the individual substance and the concentration of the substance remaining in the water. This hypothesis and the obtained rate coefficient of the individual substances were validated by simulating the kinetics of chlorine consumption and TCM formation with respect to BFA and BFA + HA. It was found that the model provided excellent simulation results.

ACKNOWLEDGEMENT

The work was jointly supported by the National Natural Science Foundation of China (Grant No.: 22006041); Guangdong Basic and Applied Basic Research Foundation (Grant No.: c212019102500000020, 2020A1515111128) and Guangzhou Basic and Applied Basic Research Foundation (Grant No.: 202002030169). Part of the experimental work was conducted in Dresden University of Technology, the first author thanks the support.

DATA AVAILABILITY STATEMENT

All relevant data are included in the paper or its Supplementary Information.

CONFLICT OF INTEREST

The authors declare there is no conflict.

REFERENCES

APHA 2005 *4500-Cl G: Standard Method for Determination of Chlorine (Residual)*. American Water Works Association and Water Environment Federation, Washington, D.C.

Barbot, E. & Moulin, P. 2008 Swimming pool water treatment by ultrafiltration–adsorption process. *Journal of Membrane Science* **314** (1), 50–57.

Blatchley, E. R. & Cheng, M. 2010 Reaction mechanism for chlorination of urea. *Environmental Science & Technology* **44** (22), 8529–8534.

Borgmann-Strahsen, R. 2003 Comparative assessment of different biocides in swimming pool water. *International Biodeterioration & Biodegradation* **51** (4), 291–297.

Chowdhury, S., Champagne, P. & McLellan, P. J. 2009 Models for predicting disinfection byproduct (DBP) formation in drinking waters: a chronological review. *Science of The Total Environment* **407** (14), 4189–4206.

Chowdhury, S., Alhooshani, K. & Karanfil, T. 2014 Disinfection byproducts in swimming pool: occurrences, implications and future needs. *Water Research* **53**, 68–109.

Chu, H. & Nieuwenhuijsen, M. 2002 Distribution and determinants of trihalomethane concentrations in indoor swimming pools. *Occupational and Environmental Medicine* **59** (4), 243–247.

De Laat, J., Feng, W., Freyfer, D. A. & Dossier-Berne, F. 2011 Concentration levels of urea in swimming pool water and reactivity of chlorine with urea. *Water Research* **45** (3), 1139–1146.

Fisher, I., Kastl, G. & Sathasivan, A. 2012 A suitable model of combined effects of temperature and initial condition on chlorine bulk decay in water distribution systems. *Water Research* **46** (10), 3293–3303.

Fisher, I., Kastl, G., Sathasivan, A. & Catling, R. 2021 Modelling chlorine residual and trihalomethane profiles in water distribution systems after treatment including pre-chlorination. *Journal of Environmental Chemical Engineering* **9** (4), 105686.

Goeres, D. M., Palys, T., Sandel, B. B. & Geiger, J. 2004 Evaluation of disinfectant efficacy against biofilm and suspended bacteria in a laboratory swimming pool model. *Water Research* **38** (13), 3103–3109.

Hong, H. C., Wong, M. H. & Liang, Y. 2009 Amino acids as precursors of trihalomethane and haloacetic acid formation during chlorination. *Archives of Environmental Contamination and Toxicology* **56** (4), 638–645.

Hua, P., Vasyukova, E. & Uhl, W. 2015 A variable reaction rate model for chlorine decay in drinking water due to the reaction with dissolved organic matter. *Water Research* **75**, 109–122.

Judd, S. J. & Bullock, G. 2003 The fate of chlorine and organic materials in swimming pools. *Chemosphere* **51** (9), 869–879.

Kanan, A. & Karanfil, T. 2011 Formation of disinfection by-products in indoor swimming pool water: the contribution from filling water natural organic matter and swimmer body fluids. *Water Research* **45** (2), 926–932.

Keuten, M. G. A., Peters, M. C. F. M., Daanen, H. A. M., de Kreuk, M. K., Rietveld, L. C. & van Dijk, J. C. 2014 Quantification of continual anthropogenic pollutants released in swimming pools. *Water Research* **53**, 259–270.

Keuten, M. G. A., Schets, F. M., Schijven, J. F., Verberk, J. Q. J. C. & van Dijk, J. C. 2012 Definition and quantification of initial anthropogenic pollutant release in swimming pools. *Water Research* **46** (11), 3682–3692.

Li, J. & Blatchley, E. R. 2007 Volatile disinfection byproduct formation resulting from chlorination of organic – nitrogen precursors in swimming pools. *Environmental Science & Technology* **41** (19), 6732–6739.

Lian, L., Li J, E. Y. & Blatchley, E. R. 2014 Volatile disinfection byproducts resulting from chlorination of uric acid: implications for swimming pools. *Environmental Science & Technology* **48** (6), 3210–3217.

Liviac, D., Wagner, E. D., Mitch, W. A., Altonji, M. J. & Plewa, M. J. 2010 Genotoxicity of water concentrates from recreational pools after various disinfection methods. *Environmental Science & Technology* **44** (9), 3527–3532.

Long, L., Bu, Y., Chen, B. & Sadiq, R. 2019 Removal of urea from swimming pool water by UV/VUV: the roles of additives, mechanisms, influencing factors, and reaction products. *Water Research* **161**, 89–97.

Lourencetti, C., Grimalt, J. O., Marco, E., Fernandez, P., Font-Ribera, L., Villanueva, C. M. & Kogevinas, M. 2012 Trihalomethanes in chlorine and bromine disinfected swimming pools: air-water distributions and human exposure. *Environment International* **45**, 59–67.

Manasfi, T., De Méo, M., Coulomb, B., Di Giorgio, C. & Boudenne, J.-L. 2016 Identification of disinfection by-products in freshwater and seawater swimming pools and evaluation of genotoxicity. *Environment International* **88**, 94–102.

Peng, D., Saravia, F., Abbt-Braun, G. & Horn, H. 2016 Occurrence and simulation of trihalomethanes in swimming pool water: a simple prediction method based on DOC and mass balance. *Water Research* **88**, 634–642.

Piñeiro, G., Perelman, S., Guerschman, J. P. & Paruelo, J. M. 2008 How to evaluate models: observed vs. predicted or predicted vs. observed? *Ecological Modelling* **216** (3–4), 316–322.

Plewa, M. J., Wagner, E. D., Muellner, M. G., Hsu, K.-M. & Richardson, S. D. 2008 Comparative Mammalian Cell Toxicity of N-DBPs and C-DBPs. In: Karanfil, T., Krasner, S. W., Westerhoff, P. & Xie, Y. (eds). *Disinfection By-Products in Drinking Water*. American Chemical Society, pp. 36–50.

Richardson, S. D., DeMarini, D. M., Kogevinas, M., Fernandez, P., Marco, E., Lourencetti, C., Ballesté, C., Heederik, D., Meliefste, K. & McKague, A. B. 2010 What's in the pool? A comprehensive identification of disinfection by-products and assessment of mutagenicity of chlorinated and brominated swimming pool water. *Environmental Health Perspectives* **118** (11), 1523–1530.

Sathasivan, A., Kastl, G., Korotta-Gamage, S. & Gunasekera, V. 2020 Trihalomethane species model for drinking water supply systems. *Water Research* **184**, 116189.

Shang, C. & Blatchley, E. R. 1999 Differentiation and quantification of free chlorine and inorganic chloramines in aqueous solution by MIMS. *Environmental Science & Technology* **33** (13), 2218–2223.

Virkutyte, J., Al-Abed, S. R. & Dionysiou, D. D. 2012 Depletion of the protective aluminum hydroxide coating in TiO2-based sunscreens by swimming pool water ingredients. *Chemical Engineering Journal* **191**, 95–103.

Yang, X., Peng, J., Chen, B., Guo, W., Liang, Y., Liu, W. & Liu, L. 2012 Effects of ozone and ozone/peroxide pretreatments on disinfection byproduct formation during subsequent chlorination and chloramination. *Journal of Hazardous Materials* **239–240**, 348–354.

Yeh, R. Y. L., Farré, M. J., Stalter, D., Tang, J. Y. M., Molendijk, J. & Escher, B. I. 2014 Bioanalytical and chemical evaluation of disinfection by-products in swimming pool water. *Water Research* **59**, 172–184.

Zwiener, C., Richardson, S. D., De Marini, D. M., Grummt, T., Glauner, T. & Frimmel, F. H. 2007 Drowning in disinfection byproducts? assessing swimming pool water. *Environmental Science & Technology* **41** (2), 363–372.

First received 8 June 2022; accepted in revised form 4 August 2022. Available online 11 August 2022